Evidence for Adsorption of Chlorine Species on Iron (III) (Hydr)oxides in the Sheepbed Mudstone, Gale Crater, Mars

T. S. Peretyazhko[1] [ID]**, S. J. Ralston[1], B. Sutter[1]** [ID]**, and D. W. Ming[2]** [ID]

[1]Jacobs, NASA Johnson Space Center, Houston, TX, USA, [2]NASA Johnson Space Center, Houston, TX, USA

Abstract Ancient aquatic environments in Yellowknife Bay, Gale crater, Mars, could create favorable conditions for adsorption of chlorine compounds (perchlorate and chloride) on Fe (III) (hydr)oxides present in the Sheepbed mudstone, such as akaganeite and ferrihydrite. In this work, 5.2 mM ClO_4^- and 1.7 to 12 mM Cl^- were adsorbed onto ferrihydrite and 5.2 mM ClO_4^- was adsorbed onto akaganeite at ultraacidic (pH 2–2.5), acidic (pH 3.8–4.5), and near-neutral (pH 6.2–7.7) pH. Samples were characterized by evolved gas analysis and compared to the data collected for the Cumberland sample from the Sheepbed mudstone. Evolved gas analysis showed that ferrihydrite with 0.5–1 wt.% ClO_4^- adsorbed under ultraacidic and acidic conditions had a well-resolved O_2 peak at 306 °C due to the thermal decomposition of adsorbed ClO_4^-. All akaganeite samples with 0.5 wt.% adsorbed ClO_4^- had a weak peak at 312 °C tentatively assigned to decomposing perchlorate. Evolved gas analysis demonstrated that 0.5–2 wt.% Cl^- adsorbed on ferrihydrite at ultraacidic and acidic pH was the main contributor to HCl evolved at >470 °C. Comparison with martian observations indicated that the temperature of the O_2 peak originating from ClO_4^- adsorbed on ferrihydrite matched well with the thermal evolution of O_2 from the Cumberland. Evolved HCl originating from Cl^- adsorbed on ferrihydrite was within the temperature range of the high-temperature HCl release from Cumberland (~770 °C). These observations suggest that ferrihydrite containing adsorbed ClO_4^- and Cl^- could exist in the mudstone. Experimental results are consistent with adsorption at acidic pH < 4 environments through postdepositional water-rock interactions of ferrihydrite with acid-sulfate groundwater containing dissolved chloride and perchlorate.

Plain Language Summary Chlorine species such as chloride and perchlorate are detected in Gale crater on Mars. However, the chemical nature of these species is still not well understood. We hypothesized that perchlorate and chloride could be adsorbed on Fe (III) (hydr)oxides present in Gale crater. To verify this hypothesis, we investigated adsorption on ferrihydrite and akaganeite and characterized adsorbed species with analytical techniques similar to those used on *Curiosity* rover. Our data indicate that adsorption of perchlorate and chloride on ferrihydrite is consistent with observations from Gale crater. These results can be used to constrain aqueous conditions on early Mars: Adsorption likely took place as a result of ferrihydrite interaction with acidic groundwater.

1. Introduction

Chlorine is a widespread element on Mars, present in dust, soils, and rocks, including the Sheepbed mudstone at Yellowknife Bay, Gale crater (Berger et al., 2016; Ming et al., 2008; Sutter et al., 2017). The Sheepbed mudstone was deposited in lacustrine environments of near-neutral pH and low salinity ~3.7 Ga ago (Grotzinger et al., 2014). Combined elemental and volatile analyses of two drilled samples, Cumberland and John Klein, indicated that chloride (Cl^-) and oxychlorine species, including perchlorate (ClO_4^-) and chlorate (ClO_3^-), are likely present in the mudstone (Hogancamp et al., 2018; Ming et al., 2014; Sutter et al., 2017). Oxychlorine phases have been detected by the Sample Analysis at Mars (SAM) instrument onboard the *Curiosity* rover mainly based on evolved O_2 (Glavin et al., 2013; Ming et al., 2014; Sutter et al., 2017). The presence of chlorides has been inferred from an observation that chlorine content estimated from the SAM measurements of oxychlorine compounds is always lower than the total chlorine in the mudstone measured by the Alpha Particle X-ray Spectrometer (Sutter et al., 2017).

The nature of chloride and oxychlorine species in Sheepbed mudstone is still not well constrained. It has been hypothesized that both are present as salts which could be either amorphous or crystalline but

below the detection limit of the Chemistry and Mineralogy (CheMin) X-ray diffraction (XRD) instrument (<1 wt.%, (Rampe et al., 2017; Sutter et al., 2017)). Some chloride could also be associated with akaganeite [β-FeO(OH,Cl) a chloride-containing Fe (III) (hydr)oxide] detected by the CheMin (Peretyazhko et al., 2019; Vaniman et al., 2014). Identification of oxychlorine salts has been attempted by evolved gas analysis (EGA) of analog samples run under SAM-like operating conditions in laboratory testbeds and then compared to the EGA data returned by the SAM instrument. The analysis of pure perchlorate salts and salts physically mixed with Fe (III) (hydr)oxides has not provided an unequivocal temperature match to the SAM O_2 release from the Cumberland sample (Ming et al., 2014; Sutter et al., 2015; Sutter et al., 2017). It was further demonstrated that decomposition of sodium or magnesium chlorates mixed with Fe (III) (hydr)oxides could be responsible for the evolved O_2 from the Cumberland sample (Hogancamp et al., 2018). We alternatively hypothesize that adsorbed perchlorate and chloride exist in the mudstone. The presence of water in contact with Sheepbed mudstone could have caused adsorption of ClO_4^- and Cl^- but not ClO_3^- on mudstone particle surfaces (Kumar et al., 2010; 2014; Wang et al., 1987). Chloride and perchlorate adsorption could occur, in particular, on Fe (III) (hydr)oxide phases as supported by laboratory observations on terrestrial materials (Kumar et al., 2010; Kumar et al., 2014; Wang et al., 1987). Chlorate can be adsorbed on activated carbon or calcium carbonate (Li et al., 2015; Mahmudov & Huang, 2011), but it has not been shown to adsorb on Fe (III) (hydr)oxides.

Mineralogical and compositional analyses of the drilled Cumberland sample revealed the presence of several Fe (III) (hydr)oxides in Sheepbed mudstone. Small amounts of akaganeite (1 wt.%) were detected in the sample (Morrison et al., 2018). The sample also contained ~30 wt.% of Fe-rich X-ray amorphous phase(s) (Vaniman et al., 2014). Such Fe enrichment was proposed to be due to the presence of ferrihydrite which could be similar to nanophase Fe oxide reported in Gusev crater and Meridiani Planum (Dehouck et al., 2014; Morris et al., 2004). The presence of liquid water and Fe (III) (hydr)oxides could therefore create favorable conditions for adsorption to occur. As a result, chlorine species adsorbed on Fe (III) (hydr)oxides might exist in the Sheepbed mudstone but so far could not be confirmed. Characterization of these adsorbed species with instruments similar to mission instruments and laboratory experiments on martian analog materials is necessary to identify adsorbed chlorine species in the mudstone.

The objectives of this work were to determine adsorption of perchlorate and chloride on ferrihydrite and perchlorate on akaganeite and to enable data comparison by characterizing adsorbed chloride and perchlorate with thermal analysis (TA) and EGA run under operating conditions similar to the SAM instrument. The laboratory data were compared to evolved O_2 and HCl results collected for the drilled Cumberland sample to evaluate the presence of adsorbed chlorine species.

2. Materials and Methods

2.1. Starting Materials

A stock solution of 0.7 M perchlorate was prepared by dissolving $NaClO_4 \cdot H_2O$ (Honeywell) in MilliQ ultrapure water. Fresh and aged ferrihydrite and fresh akaganeite were used in adsorption experiments. Akaganeite was identified by XRD analysis of Cumberland sample, and ferrihydrite has been suggested as a component in the X-ray amorphous phase(s) in Gale crater samples (Dehouck et al., 2014; Peretyazhko et al., 2018). Both akaganeite and ferrihydrite adsorb anions, and poorly crystalline akaganeite has been previously shown to adsorb perchlorate (Kumar et al., 2010; Kumar et al., 2014). Fresh ferrihydrite was used within 3 months after synthesis. Aged ferrihydrite was stored for 3 years under lab ambient conditions prior to adsorption experiments (~17 °C and 65% relative humidity measured by Vaisala MI70 humidity meter with DMP74A probe). Ferrihydrite aging causes mineralogical and morphological changes including formation of small amounts of hematite (see section 3.1). Hematite, at the CheMin detection limit, was reported in Sheepbed mudstone from the Cumberland drill site (Vaniman et al., 2014). Therefore, aged ferrihydrite with traces of hematite could be a better match to ferrihydrite in Cumberland sample which likely formed when abundant water was present in Gale crater then matured with time and partially transformed into hematite. For akaganeite adsorption experiments, only freshly prepared akaganeite was used because aging in air has not been shown to affect its mineralogy or crystallinity (Luna et al., 2014). It should be noted that mineralogical analyses demonstrated that Cumberland sample contained other potential adsorbents, including smectite and basaltic glass (Dehouck et al., 2014; Vaniman et al., 2014). These phases were not included to study adsorption of chlorine species because of their negligible anion adsorption capacity (Dultz et al., 2016;

Meunier, 2005). Smectites have permanent negative structural charge which causes anion repulsion (Meunier, 2005). Adsorption of chloride and perchlorate on mineral surfaces is larger under acidic than neutral or alkaline conditions (Chubar et al., 2005; Kumar et al., 2010; Lien et al., 2010; Wang et al., 1987). However, basaltic glass dissolves under acidic conditions and its dissolution is accompanied by increase in solution pH up to neutral/alkaline pH values resulting in low anion adsorption (Dultz et al., 2016).

Ferrihydrite was prepared by grinding a mixture of 20 g Fe $(NO_3)_3 \cdot 9H_2O$ and 12 g NH_4HCO_3 (1.7:1 mass ratio) for 15 min until CO_2 bubbling ceased and brown precipitate formed (Smith et al., 2012). The resulting slurry was dried at 100 °C for 24 hr, rinsed, and vacuum filtered with three 50 mL portions of ultrapure water and then dried at 70 °C. Prior to adsorption experiments, both fresh and aged ferrihydrite samples were washed at pH 11. Alkaline washing was performed in order to remove any residual nitrate which can outcompete perchlorate for adsorption sites (Rietra et al., 2000). For alkaline washing, 1 g of ferrihydrite was suspended in 50 mL ultrapure water and stirred. While stirring, 1 M NaOH was added to raise the pH to pH ~11. The suspension was allowed to equilibrate for ~5 min and then centrifuged at 26,000 rpm for 5 min. The solids were then washed thrice with deionized water and air dried. The residual nitrate in the air-dried ferrihydrite samples was monitored as NO gas released during TA/EGA. The analysis of the samples after alkaline treatment demonstrated little NO release with respect to the unwashed sample (Figure S1 in the supporting information). Akaganeite was prepared by hydrolysis of 0.2 M $FeCl_3$ at 80 °C for 5 hr (Ståhl et al., 2003). The suspension was cooled overnight, and the supernatant was removed. The precipitated akaganeite was washed twice with deionized water and air dried.

Mineralogy of the synthesized oxides was checked with XRD and evolved gases of O_2, H_2O, and HCl by TA/EGA as described in section 2.3. Surface area was determined by N_2-BET method with a Micromeritics TriStar II 3020 surface area and porosity instrument. Prior to analysis, akaganeite and ferrihydrite samples were heated overnight under vacuum at 150 °C to remove adsorbed water. It should be noted that both NaOH-washed and unwashed fresh ferrihydrite were analyzed. The amount of the washed aged ferrihydrite was insufficient for BET analysis, and therefore, only the unwashed sample was measured. The analysis of the surface area of the fresh ferrihydrite showed that the surface area decreased by ~20 m^2/g after washing from 316 to 298 m^2/g, and similar decrease in the surface area might occur for the aged ferrihydrite.

2.2. Adsorption Experiments

Suspensions of 6.7 g/L ferrihydrite or akaganeite were prepared by mixing 200 mg solid phase with 29.8 mL ultrapure water in 60-ml plastic bottles. A small volume of 1 M HCl or NaOH was added to the stirred suspensions to reach ultraacidic (pH 2–2.5), acidic (pH 3.8–4.5), and near-neutral (pH 6.2–7.3) pH conditions (Figure 1 and Table 1). Iron (III) (hydr)oxide surface remains positively charged at this pH range since the selected pH interval was below the point of zero charge (pzc) reported in the literature (pH$_{pzc}$ is value at which surface charge is equal to 0; ferrihydrite pH$_{pzc}$ is 7.2–8 (Hsi & Langmuir, 1985; Kosmulski, 2002), and akaganeite pH$_{pzc}$ is ~7.9 (Parida et al., 1997)). Perchlorate adsorption in the presence of chloride, added as HCl to obtain ultraacidic and acidic pH, could match aquatic geochemical processes that likely occurred in ancient mudstone as samples from Gale crater contain both oxychlorine and chloride species (Sutter et al., 2017). Three replicates were prepared for each pH range. The samples were equilibrated without shaking for 24 hr then an aliquot of $NaClO_4$ stock solution was added to achieve a perchlorate concentration of 5.2 mM. The suspensions were stirred during perchlorate addition. After perchlorate addition, the samples were equilibrated without shaking for 24 hr. Samples were not shaken in order to mimic natural undisturbed conditions. In addition, our preliminary experiments demonstrated that shaking did not affect the amount of adsorbed perchlorate. An ~2 mL aliquot was collected and filtered (<0.22 μm) immediately after ClO_4^- addition, and the second aliquot was taken after 24 hr equilibration. The collected samples were analyzed by ion chromatography for dissolved Cl^- and ClO_4^-. Suspension pH was checked right after ClO_4^- addition and at the end of adsorption experiment. At the end of experiments, the solids were separated from supernatant by centrifugation, washed twice with ultrapure water, and air dried for XRD and TA/EGA. Washing was necessary to remove any residual perchlorate and chloride salts to ensure that samples used for TA/EGA contained only adsorbed chloride and perchlorate. The procedure might also cause anion desorption if pH increases to near-neutral conditions during washing and release of chloride from akaganeite tunnels (Peretyazhko et al., 2019).
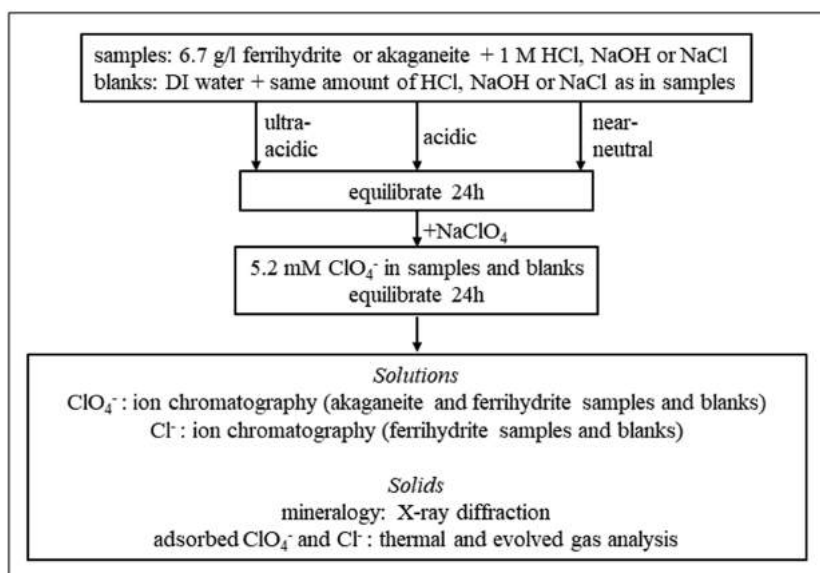
Figure 1. Flowchart of adsorption experiments. Adsorption experiments with NaCl were used to study Cl⁻ adsorption under near-neutral pH conditions, and NaClO₄ was not added to these samples and blanks.

Addition of 1 M HCl to maintain ultraacidic and acidic pH conditions also provided Cl⁻ in solution along with ClO_4^- for adsorption on the solids. Adsorbed chloride was measured in ferrihydrite suspensions which contained 10 and 11.7 mM total Cl⁻ in the ultraacidic fresh and aged ferrihydrite, respectively, and 1.7 mM total Cl⁻ in both acidic ferrihydrite samples. In order to extend chloride adsorption to near-neutral pH conditions, 1 M NaCl was used as a source of Cl⁻ (Figure 1). Experiments were performed only with fresh ferrihydrite. The amount of available aged ferrihydrite was insufficient to perform this experiment. An aliquot of NaCl stock solution was added to match the amount of Cl⁻ added as HCl in the ultraacidic and acidic samples. After 24 hr equilibration, the pH was around 7.65 ± 0.05 and close to near-neutral pH conditions (Table 1). Chloride adsorption on akaganeite was not determined because of the contribution of akaganeite tunnels to chloride uptake and/or release which changes with pH and complicates quantification of adsorbed Cl⁻ (Kozin & Boily, 2013; Peretyazhko et al., 2019).

Three blanks were prepared the same way as the samples, but no Fe (III) (hydr)oxide was added (Figure 1). The amounts of HCl, NaOH, NaCl, and NaClO₄ stock solutions as well as sampling procedures for ion chromatography were exactly the same as in the corresponding ferrihydrite- and akaganeite-containing samples.

2.3. Characterization

Iron (III) (hydr)oxides before and after adsorption experiments were analyzed by XRD and TA/EGA. Powder samples were placed on zero background slides for XRD analysis and analyzed at 45 kV and 40 mA with a 0.02° 2θ step and 1 min time per step using a Panalytical X'Pert Pro instrument (Co Kα radiation). The instrument was operated under ambient conditions and calibrated with a novaculite standard (Gemdugout, State College, PA).

TA/EGA was performed with a Labsys Evo Simultaneous Thermal Analysis instrument (Setaram Instrumentation, KEP Technologies) connected to a quadrupole mass spectrometer (Thermostar GSD 320, Pfeiffer Vacuum Incorporated). The instrument was configured to operate similarly to the SAM instrument, and measurements were performed with a ramp rate of 35 °C/min, furnace pressure of 30 mbar, flow rate of 10 sccm, maximum temperature of 1000 °C, and helium carrier gas (Archer et al., 2014). Approximately 10 mg sample was used for analyses, and three replicates were run. The Fe (III) (hydr)oxide samples analyzed for adsorbed Cl⁻ and/or ClO_4^- are shown in Table 2. Pure NaClO₄ salt

Table 1

The Values of pH Corresponding to Ultraacidic, Acidic, and Near-Neutral pH Ranges at the End of ClO_4^- and Cl⁻ Adsorption Experiments (pH_{24h})

Fe (III) (hydr)oxide	Ultraacidic	Acidic	Near-neutral
Fresh ferrihydrite	2.50 ± 0.02	4.51 ± 0.02	6.92 ± 0.06
			7.65 ± 0.05[a]
Aged ferrihydrite	2.27 ± 0.05	4.23 ± 0.07	7.28 ± 0.05
Akaganeite	2.00 ± 0.04	3.78 ± 0.40	6.42 ± 0.01

[a]pH measured in Cl⁻ adsorption experiments in which NaCl was used as a source of Cl⁻.

Table 2
Iron (III) (Hydr)oxide Samples and Controls Analyzed by Thermal and Evolved Gas Analyses

Aged ferrihydrite	Fresh ferrihydrite	Akaganeite
Samples analyzed for adsorbed Cl⁻ and ClO₄⁻		
Ultraacidic	Ultraacidic	
Acidic	Acidic	
Samples analyzed for adsorbed ClO₄⁻		
Near-neutral	Near-neutral	Ultraacidic
		Acidic
		Near-neutral
Controls analyzed for adsorbed Cl⁻		
Acidic	Acidic	

used to prepare a perchlorate stock solution and unreacted Fe (III) (hydr) oxides was also analyzed. Acidic aged and fresh ferrihydrite controls that contained no ClO_4^- (Table 2) were prepared to evaluate evolved HCl from adsorbed Cl⁻ alone. Controls were not prepared for akaganeite because added HCl could be incorporated into tunnels. In order to synthesize acidic ferrihydrite controls, HCl of the same amount as in the acidic ClO_4-reacted ferrihydrite experiments (1.7 mM) was added to 6.7 g/L suspensions of the aged and fresh ferrihydrite. The controls were equilibrated for 24 hr; the solids were separated from supernatant by centrifugation, washed twice with ultrapure water, and air dried. The amount of adsorbed chloride determined as described below was 128 μmol/g (0.4 wt.%) and 194 μmol/g (0.7 wt.%) for the aged and fresh acidic ferrihydrite, respectively.

Adsorbed ClO_4^- and Cl⁻ were determined with ion chromatography. Ion chromatography analysis was performed with a Dionex ICS-2000 instrument equipped with a Dionex IonPac AS18 column (4×250 mm), Dionex EGC III KOH eluent, and a suppressed conductivity detector Dionex AERS 500 with a 20-μL injection volume. Aqueous perchlorate was analyzed in the samples and blanks (no Fe (III) hydroxides added). Adsorbed perchlorate was calculated as a difference between aqueous perchlorate in the blanks and in the samples equilibrated for 24 hr. Adsorbed chloride was calculated the same way as adsorbed perchlorate. It should be noted that adsorption of Na^+, added as $NaClO_4$, NaOH and/or NaCl, was not measured because Na^+ does not adsorb in the pH range from ~2 to ~7.6 (i.e., pH close to or below pH_{pzc}) when Fe (III) (hydr)oxide surfaces are positively charged or the charge is close to 0 (Dumont & Watillon, 1971).

3. Results

3.1. Characterization of Fe (III) (Hydr)Oxides

The freshly synthesized ferrihydrite was two-line ferrihydrite as evidenced by two broad XRD peaks for the 110 (~40° 2θ) and 115 (70° 2θ) crystal planes (Figure 2a) (Schwertmann et al., 1999). Three-year aged ferrihydrite sample was also two-line ferrihydrite but contained traces of hematite based on the presence of small 012 (28.1° 2θ), 104 (38.6° 2θ), and 116 (63.6° 2θ) peaks and slight sharpening of the 110 ferrihydrite diffraction peak (Figure 2a). The amount of hematite determined by Rietveld refinement was ~2 wt.%. Lack of hematite in the fresh ferrihydrite indicated that it formed during ferrihydrite storage under ambient conditions. The appearance of hematite in aged ferrihydrite was likely caused by humidity in our lab (65% relative humidity). The process has been previously shown to occur for air-dried ferrihydrite in the presence of small amounts of water, and the rate of transformation increases with humidity (Schwertmann et al., 1999; Torrent et al., 1982). Formation of hematite likely proceeded through aggregation of ferrihydrite particles followed by hematite interface nucleation and crystal growth (Fischer & Schwertmann, 1975; Soltis et al., 2016). XRD analysis of the synthesized akaganeite revealed the sole presence of crystalline akaganeite, with no traces of other oxides (Figure 2b). Analysis of Fe (III) (hydr)oxide phases at the end of adsorption revealed that no mineralogical changes occurred under experimental conditions (data not shown).

Surface areas for unwashed fresh and aged ferrihydrite as well as akaganeite determined by the BET method are reported in Table 3. Surface area of fresh ferrihydrite and akaganeite (Table 3) was within the range reported in the literature (33–280 m^2/g for akaganeite and 180–340 m^2/g for ferrihydrite (Cornell & Schwertmann, 2003; Mazeina et al., 2006)). A decrease in the surface area from 316 to 206 m^2/g was observed between fresh and aged ferrihydrite (Table 3). The decrease was a result of increased ferrihydrite aggregation that makes internal surfaces inaccessible for N_2 adsorption (Cornell & Schwertmann, 2003). Partial crystallization of ferrihydrite to hematite (Figure 2a) also caused loss in surface area (Cornell & Schwertmann, 2003).

EGA of the initial Fe (III) (hydr)oxides showed H_2O release in the temperature range of 50–800 °C due to escape of adsorbed water and dehydroxylation. The H_2O peak was at 150–160 °C for the fresh and aged ferrihydrites and at 215 °C for akaganeite (Figure S2). Small O_2 peaks were observed around the same temperatures as H_2O peaks (Figure S2). These evolved O_2 peaks were related to decomposition of water into O_2 and
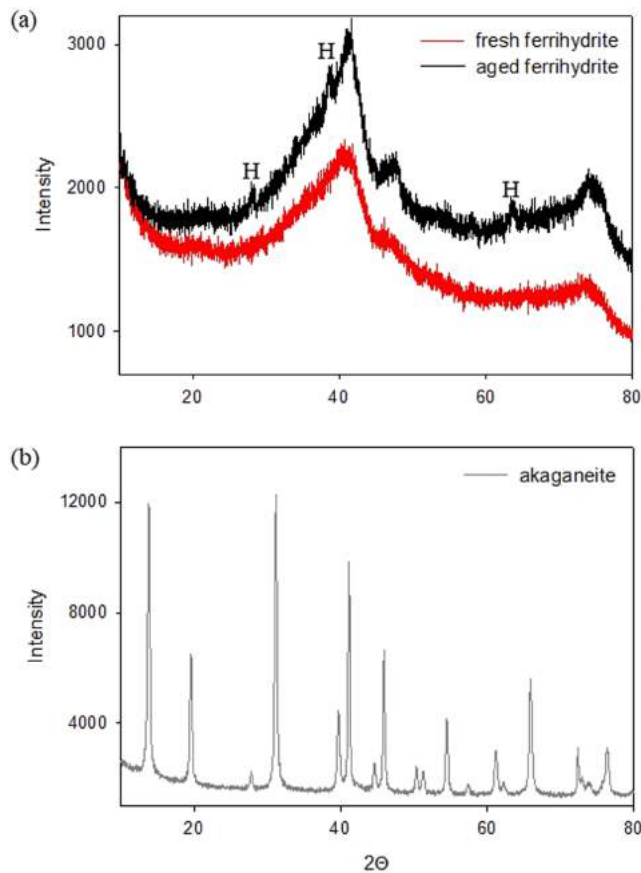
Figure 2. X-ray diffraction of unreacted: (a) fresh and 3-year aged ferrihydrite and (b) akaganeite.

H_2, because H_2 release followed the same trend as water and oxygen (Figure S3). During thermal decomposition of akaganeite, HCl was evolved between 300 and 600 °C and had overlapping peaks around 350, 420, and 500 °C (Figure S2c). The released HCl originated from collapsing akaganeite tunnels and/or from the surface of the forming hematite ((Peretyazhko et al., 2019, and references therein).

3.2. Perchlorate and Chloride Adsorption on Fe (III) (Hydr)oxides

Perchlorate and chloride adsorption was investigated under three pH conditions: ultraacidic (pH 2–2.5), acidic (pH 3.8–4.5), and Near-neutral (pH 6.2–7.7). The pH remained unchanged during 24 hr equilibration after perchlorate and/or chloride addition (Tables 1 and S1). The amount of adsorbed perchlorate on ferrihydrite and akaganeite varied from 0.2 to 1.2 wt.% (Figure 3a) which was within the range of perchlorate contents in Gale crater (0.050 ± 0.025 to 1.05 ± 0.44 wt.%, (Sutter et al., 2017)). Adsorbed chloride in ferrihydrite suspensions (0.3–2.2 wt.%, Figure 3b) was within the range or higher than total chlorine content in Gale crater (0.29 ± 0.09 to 1.19 ± 0.36 wt.% (Sutter et al., 2017)).

Perchlorate adsorption varied with pH in the fresh and aged ferrihydrite suspensions. The amount of adsorbed ClO_4^- decreased as pH changed from acidic to ultraacidic conditions. Adsorbed perchlorate was ~120 µmol/g (1.2 wt.%) and ~50 µmol/g (0.5 wt.%) at acidic and ultraacidic pH, respectively, for both ferrihydrite samples (Figure 3a). Perchlorate adsorption occurred solely through electrostatic interactions with positively charged hydroxyl groups (Sparks, 2003). Therefore, larger ClO_4^- adsorption would be expected at lower pH, as ferrihydrite surface becomes more positively charged (Kumar et al., 2010; Lien et al., 2010). The lower ClO_4^- adsorption under ultraacidic than acidic conditions was likely caused by chloride adsorption (0.3–2.2 wt.%, Figure 3b) added as HCl for pH adjustments in acidic and ultraacidic ferrihydrite samples.

Chloride has higher affinity for adsorption surface sites and outcompetes perchlorate likely due to Cl^- adsorption by two different mechanisms, electrostatic interactions and covalent bonding (Acelas & Flórez, 2018; Bourikas et al., 2001; Rietra et al., 2000; Wang et al., 1987; Zhang et al., 1996). Chloride adsorption has been shown to increase with pH decrease (Chubar et al., 2005; Wang et al., 1987), and, as a result, larger Cl^- adsorption in ultraacidic samples (Figure 3b) could suppress ClO_4^- adsorption. Suppression of ClO_4^- adsorption in the presence of Cl^- was confirmed by an increase in perchlorate adsorption on ferrihydrite to which $HClO_4$ instead of HCl was added. The results revealed that ~400 µmol/g ClO_4^- (4 wt.%) was adsorbed on fresh ferrihydrite under ultraacidic conditions (Table S2).

When pH reached near-neutral conditions in the ferrihydrite samples, the adsorbed perchlorate decreased to ~25 µmol/g (0.2 wt.%) in the aged ferrihydrite and completely disappeared in the fresh ferrihydrite

Table 3
BET Surface Area and Surface Area Normalized Amounts of Adsorbed ClO_4^- and Cl^-

Fe (III) (hydr)oxide	Surface area, m²/g	Adsorbate, µmol/m²	Ultraacidic	Acidic	Near-neutral
Fresh ferrihydrite	316.0	ClO_4^-	0.23 ± 0.06	0.38 ± 0.05	nd[a]
		Cl^-	2.01 ± 0.06	0.51 ± 0.06	nd[a]
Aged ferrihydrite	205.7	ClO_4^-	0.24 ± 0.06	0.59 ± 0.02	0.12 ± 0.04
		Cl^-	2.41 ± 0.36	0.43 ± 0.13	
Akaganeite	136.3	ClO_4^-	0.33 ± 0.07	0.38 ± 0.06	0.18 ± 0.07

Note. Adsorbed Cl^- was determined in the ultraacidic and acidic fresh and aged ferrihydrite in which pH was adjusted by 1 M HCl and in the near-neutral fresh ferrihydrite samples to which 1 M NaCl was added as a source of Cl^-. Adsorbed Cl^- was not determined in the akaganeite samples because of the contribution of akaganeite tunnels to Cl^- uptake and/or release which complicates quantification of adsorbed Cl^-.
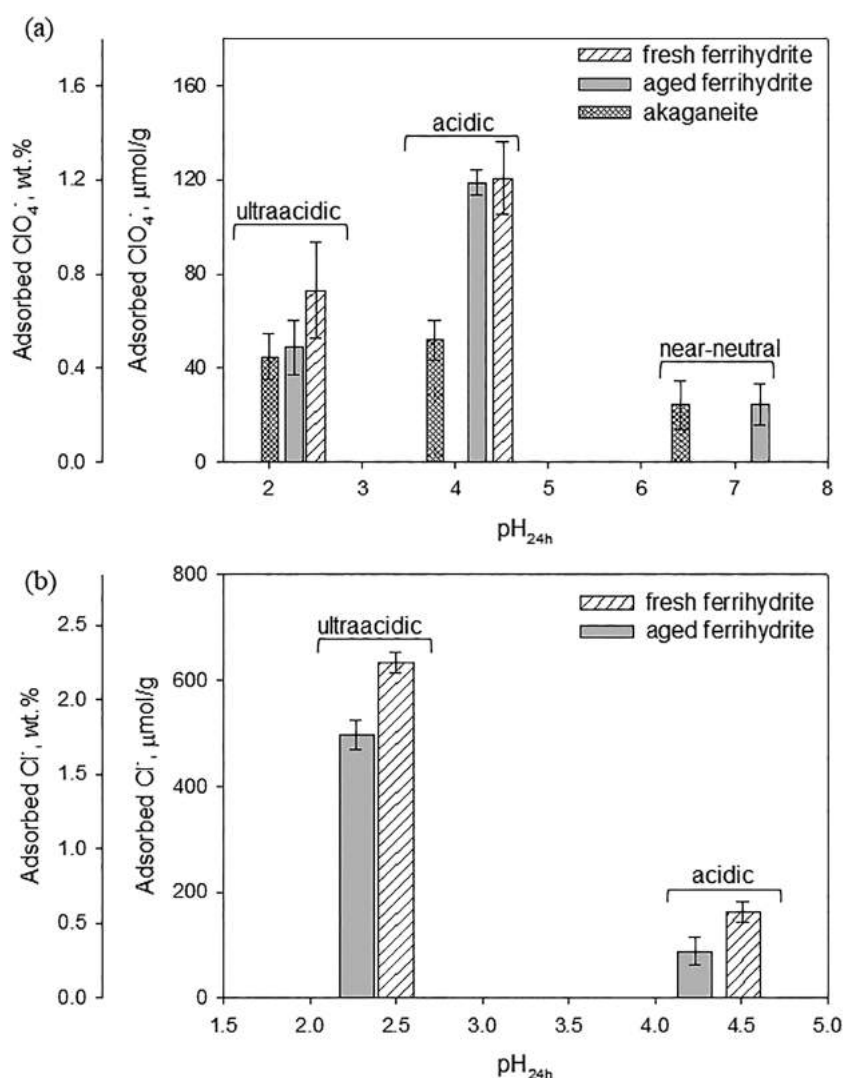[a]nd, not detected.

Figure 3. Adsorbed (a) perchlorate and (b) chloride as a function of pH measured after 24 hr ClO_4^- adsorption (pH_{24h}). No adsorbed chloride was detected under near-neutral conditions. Ultraacidic, acidic, and near-neutral pH ranges are shown.

(Figure 3a). A similar decrease in adsorbed ClO_4^- in near-neutral and alkaline conditions was observed for perchlorate adsorption on granular ferric (hydr)oxide (Kumar et al., 2010) and aluminum (hydr)oxide (Lien et al., 2010). Lower adsorption was caused by a decrease in positively charged surface sites as pH was approaching pH_{pzc}. The lack of detection of adsorbed perchlorate in the fresh ferrihydrite at near-neutral pH (Figure 3a) was presumably due to the lower pH_{pzc} of fresh than aged ferrihydrite. The pH_{pzc} values were not measured in this work; however, a slightly higher pH_{pzc} has been previously reported in aged ($pH_{pzc} \sim 8.25$) than in fresh ferrihydrite ($pH_{pzc} \sim 8.1$) (Hiemstra & Van Riemsdijk, 2009). The difference might be related to the changes in abundances of surface sites during ferrihydrite aging (Hiemstra & Van Riemsdijk, 2009). Chloride adsorption on fresh ferrihydrite did not occur under near-neutral conditions (experiments were performed with NaCl as a source of Cl^- at pH_{24h} 7.65 ± 0.05) which agreed with previous observations (Chubar et al., 2005; Wang et al., 1987).

Perchlorate adsorption on akaganeite was the same within the standard error for ultraacidic and acidic pH ranges and averaged ~50 μmol/g (0.5 wt.%, Figure 3a). The lack of pH effect on perchlorate adsorption at ultraacidic and acidic pH could be due to the presence of adsorbed chloride that suppressed perchlorate adsorption (Chambaere & Degrave, 1984). Similar to ferrihydrite, an increase in pH from acidic to neutral conditions led to a slight decrease in adsorbed perchlorate (24 μmol/g, 0.2 wt.%). Surface area normalized
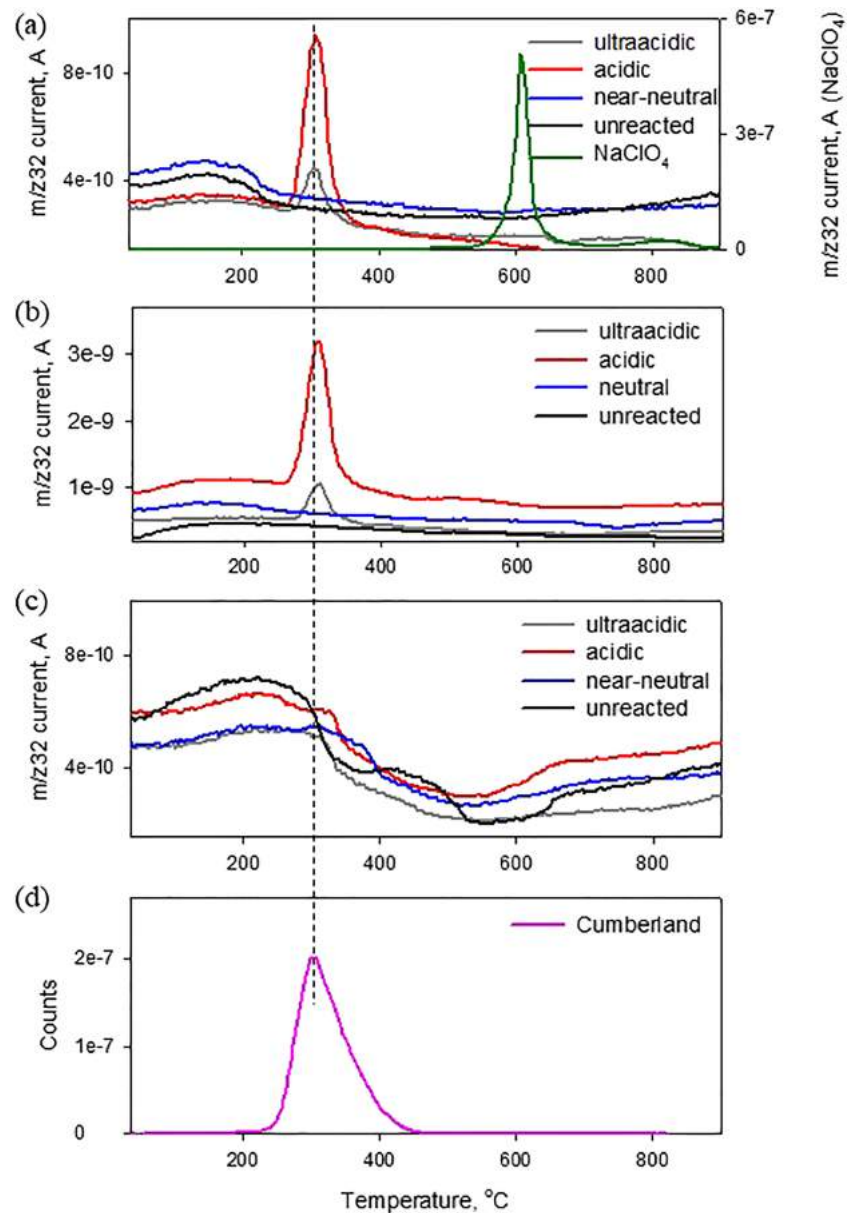
Figure 4. Evolved O_2 (m/z32) for unreacted and ClO_4-reacted (a) fresh ferrihydrite, (b) aged ferrihydrite, and (c) akaganeite. (d) O_2 release detected by SAM in Cumberland sample drilled in Yellowknife Bay, Gale crater. Evolved O_2 for the solid $NaClO_4$ is shown in (a). Dotted line shows temperature of O_2 peak in Cumberland.

amounts of adsorbed perchlorate revealed no large difference in perchlorate surface densities between akaganeite and ferrihydrite (Table 2). The results could indicate that both Fe (III) (hydr)oxides have similar densities of protonated surface sites that adsorbed ClO_4^- through electrostatic interactions.

3.3. EGA: O_2

Fresh and aged ferrihydrite samples with ClO_4^- adsorbed under ultraacidic and acidic pH conditions had an O_2 peak at 306 ± 1 °C which was not observed in the unreacted ferrihydrite (Figures 4a and 4b). The evolved O_2 peak intensity was lower in the ultraacidic than in the acidic sample, in agreement with smaller ClO_4^- adsorption under this pH condition (Figures 3a, 4a, and 4b). Based on these observations, the 306 °C peak was assigned to thermal decomposition of adsorbed perchlorate. Oxygen release at 306 °C was not detected in the aged ferrihydrite sample incubated under near-neutral conditions indicating that EGA was not

sensitive to perchlorate content of ~0.2 wt.% (Figure 4b). Evolved O_2 was also not observed in the near-neutral fresh ferrihydrite in which no adsorbed ClO_4^- was detected (Figures 3a and 4a).

Very weak O_2 peaks were also detected in all perchlorate-containing akaganeite samples, and the peaks were shifted to slightly higher temperatures (312 ± 4 °C, Figure 4c). It should be noted that the ultraacidic akaganeite sample had about the same amount of adsorbed perchlorate as both ferrihydrite samples under this pH condition (Figure 3a); however, O_2 release was much weaker (Figure 4c). The low release might be caused by partial perchlorate removal during washing steps, sample heterogeneity, and/or consumption of released O_2 during thermal analysis that resulted in the decomposition of akaganeite to hematite. Because of the weak signal strength, the O_2 peak at 312 °C in all akaganeite samples was tentatively assigned to decomposing perchlorate. Additional studies with higher perchlorate loadings are necessary to confirm it.

The temperature of the oxygen peak from thermally decomposing adsorbed perchlorate was ~290 °C lower than from solid $NaClO_4$ (Figure 4a). EGA of solid $NaClO_4$ showed release of O_2 with an intensive peak at 600 °C (Figure 4a) consistent with $NaClO_4$ thermal decomposition into $NaCl$ (Shimada, 1992):

$$NaClO_4 \rightarrow NaCl + O_2$$
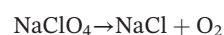
Lower temperature of O_2 release for adsorbed perchlorate indicated that adsorption on Fe (III) (hydr)oxides had a catalytic effect on perchlorate decomposition by accelerating the process. Lowering of perchlorate decomposition temperatures has been previously observed in physical mixtures with Fe (III) (hydr)oxides but not for adsorbed perchlorate (Sutter et al., 2015; Zhang et al., 1996). Catalysis in physical mixture involves formation of a surface complex between iron (III) and perchlorate which weakens bonds in the perchlorate ion and facilitates its decomposition (Zhang, Kshirsagar, et al., 1996). We hypothesize that formation of the surface complexes through perchlorate adsorption from solution might have a similar effect on the strength of chemical bonds in ClO_4^-.

3.4. EGA: HCl

Evolved HCl was detected in the ultraacidic and acidic aged ferrihydrite samples and likely originated from desorption of Cl^- but not ClO_4^-. In order to determine the origin of the evolved HCl, the thermal behavior of HCl was compared for aged ferrihydrite samples, acidic aged ferrihydrite control (no added ClO_4^-), and solid $NaClO_4$ (Figures 5 and S4). The continuous HCl release in the aged ferrihydrite samples occurred at >470 °C which was higher than the temperature of O_2 release (Figures 4b and 5b). The ultraacidic sample had two broad overlapping HCl peaks at ~680 and ~830 °C, while the acidic sample had a peak at ~620 °C (Figure 5b). A wide temperature range of HCl release in the samples was similar to the acidic aged ferrihydrite control (Figure 5b). At the same time, the HCl release pattern in the samples differed from HCl release from $NaClO_4$ with two discrete peaks at 600 and 800 °C (Figures 5a and 5b). Similarity of evolved HCl in the ultraacidic and acidic aged ferrihydrite samples and acidic aged ferrihydrite control indicated that adsorbed chloride was the main contributor to the released HCl. The chloride formed through decomposition of adsorbed perchlorate likely remained trapped in the samples; however, more detailed studies are needed to confirm it. Comparison of the evolved HCl feature for acidic aged ferrihydite sample and the control also showed that the shape of HCl release was different despite the fact that the same amount of HCl was added to both (Figure 5b). The control had two broad HCl peaks at ~620 and 800 °C, while the acidic ferrihydrite sample had one peak at 620 °C (Figures 5 and S4). The results could suggest that the presence of adsorbed perchlorate affected chloride surface distribution and thermal behavior. Further studies are necessary to fully understand the fate of adsorbed perchlorate and chloride during thermal decomposition.

The release of HCl did not occur in the ultraacidic and acidic fresh ferrihydrite samples and controls in contrast to the aged ferrihydrite (Figures 3b, 5a, and S5). Lack of HCl release is likely due to different Cl^- desorption behavior caused by ferrihydrite aging. Chloride desorption could be triggered by pH increase in solution to near-neutral conditions (Kumar et al., 2010; Wang et al., 1987) or thermal treatments (Figure 5b). Exposure of the aged and fresh ferrihydrites containing adsorbed Cl^- to near-neutral pH conditions revealed that about the same amount of Cl^- (~60%) was desorbed from both ferrihydrite samples (Table S3). The results indicate that aging did not cause changes in stability of adsorbed chloride under
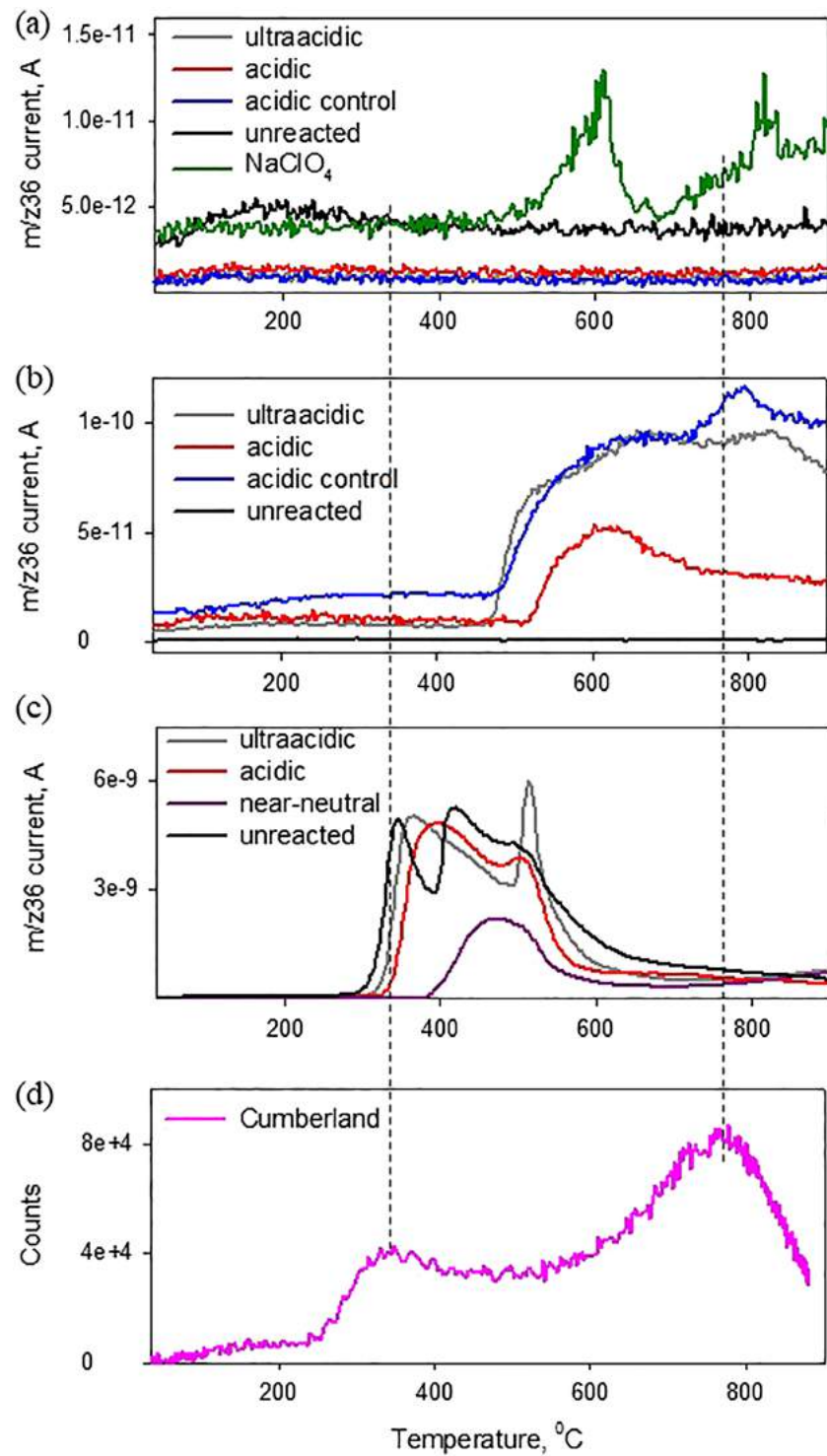
Figure 5. Evolved HCl (m/z36) for (a) fresh ferrihydrite, (b) aged ferrihydrite, and (c) akaganeite before and after adsorption experiments. (d) HCl release detected by SAM in Cumberland. Dotted lines show temperatures of HCl peaks in the drilled Cumberland sample.

aqueous conditions. We, therefore, hypothesized that ferrihydrite aging and transformation into hematite (Figure 2a) could cause a decrease in thermal stability of adsorbed Cl^- complexes resulting in the HCl release from the aged but not from the fresh ferrihydrite.

All akaganeite samples with adsorbed perchlorate had HCl release in the temperature interval from 350 to 600 °C (Figures 5c and S6). Given the weak O_2 releases from decomposition of adsorbed perchlorate (Figure 4c), ClO_4^- contribution to evolved HCl was likely negligible. The released HCl originated from Cl^- that escaped from collapsing akaganeite tunnels during the heating (Peretyazhko et al., 2019). Intensity of HCl release in the near-neutral sample was lower than in the acidic and ultraacidic samples (Figure 5c) due to larger amount of chloride release from akaganeite tunnels during incubation at higher pH values (Peretyazhko et al., 2019).

4. Discussion

4.1. Presence of Adsorbed Perchlorate and Chloride in Sheepbed Mudstone

Evolved O_2 measured by the SAM instrument in the Cumberland sample from Sheepbed mudstone had a peak at 310 °C (Figure 4d) assigned to the presence of up to ~1 wt.% oxychlorine phases (perchlorates and/or chlorates (Hogancamp et al., 2018; Ming et al., 2014; Sutter et al., 2017)). However, studies of various perchlorates revealed that the O_2 peak temperature in Cumberland sample did not agree with pure perchlorate salts as it was lower than Ca, Mg, Na, and K perchlorates (~440 to ~480 °C) and higher than Fe (II) and Fe (III) perchlorates (~200 and ~280 °C, (Glavin et al., 2013; Ming et al., 2014)). Perchlorates physically mixed with Fe phases present in Sheepbed mudstone (e.g., hematite, ferrihydrite, and magnetite) still did not match O_2 Cumberland data (Sutter et al., 2015). However, it has been shown that physical mixtures of sodium or magnesium chlorate with ferrihydrite have an O_2 peak close to the O_2 peak detected in Cumberland sample (Hogancamp et al., 2018).

Our results suggest that the oxychlorine compound responsible for the 310 °C O_2 peak in the Cumberland sample is attributed to perchlorate adsorbed on ferrihydrite. Ultraacidic and acidic samples of ferrihydrite with adsorbed perchlorate had an O_2 peak at 306 °C, while akaganeite samples had a weak O_2 peak at 312 °C tentatively assigned to perchlorate decomposition (Figure 4c). Minor amounts of akaganeite (1 wt. %) were detected in the Cumberland sample (Morrison et al., 2018). The exact amount of ferrihydrite that could exist in the mudstone is unknown; however, it can reach up to ~30 wt.% corresponding to the content of X-ray amorphous phase(s) (Vaniman et al., 2014). If both ferrihydrite and akaganeite with adsorbed perchlorate are present together then, given the potentially higher abundance of ferrihydrite than akaganeite in the Cumberland sample and weak evolved O_2 signal from akaganeite, the O_2 release from akaganeite will be overpowered by O_2 evolved from perchlorate adsorbed on ferrihydrite. We, therefore, propose that evolved O_2 detected by SAM in the Cumberland sample mainly originated from ClO_4^- adsorbed on ferrihydrite or ferrihydrite-like phase.

The Cumberland sample had an HCl release in the 250–800 °C temperature interval with two peaks at ~340 and ~770 °C (Figure 5d). The evolved HCl was proposed to originate from several sources. Thermally decomposing Cl-containing akaganeite could contribute to evolved HCl in the Cumberland sample over the whole temperature interval (Peretyazhko et al., 2019). The low-temperature HCl evolution was also proposed to be due to decomposition of Mg perchlorate and Mg chlorate alone or in a mixture with Fe (III)-containing minerals (Hogancamp et al., 2018; Sutter et al., 2017). The high-temperature peak could be due to reaction of water vapor with melting chlorides and/or decomposition of chlorates and perchlorates mixed with phyllosilicates (Clark et al., 2019; Hogancamp et al., 2018; Sutter et al., 2017).

The high-temperature HCl release in the Cumberland sample was also within the temperature range of evolved HCl originating from the aged ferrihydrite. In particular, the HCl peak position in the Cumberland sample was in between the HCl peaks observed at ~680 and ~830 °C in the ultraacidic sample (Figures 5b and 5d). Discrepancies in the exact peak position and shape between the Cumberland and the ultraacidic aged ferrihydrite samples are likely due to the presence of other minerals (e.g., smectite and basaltic glass) which can cause a shift in the HCl peak temperature in the Cumberland sample (Clark et al., 2019). Ferrihydrite, potentially present in the X-ray amorphous phase(s) in the Sheepbed mudstone deposited ~3.7 Ga ago (Grotzinger et al., 2014), would be similar to our synthetic aged ferrihydrite. The mineral likely formed when water was present in Gale crater and then matured with time. The minor amount of hematite (~0.4 wt. %) in the Cumberland sample (Morrison et al., 2018) could be a product of ferrihydrite aging similar to what happened in our laboratory aged ferrihydrite after 3 years of storage (Figure 2a).

4.2. Aqueous Conditions Required for Perchlorate/Chloride Adsorption in Yellowknife Bay

Results of adsorption experiments suggest that perchlorate and chloride adsorbed on ferrihydrite or ferrihydrite-like phase are present together only below pH 4. Adsorption in Sheepbed mudstone presumably occurred on the ferrihydrite component of the X-ray amorphous phase(s), similar to the aged ferrihydrite used in this study. Laboratory analyses indicated that ClO_4^- adsorbed under ultraacidic and acidic conditions was detected by EGA. However, EGA was not sensitive to perchlorate content of ~0.2 wt.% adsorbed under the near-neutral conditions (Figure 3a). Chloride adsorption on ferrihydrite occurred under ultraacidic and acidic but not near-neutral conditions (Figure 3b). The high-temperature HCl peak in Cumberland sample (770 °C) was within the range of HCl peaks in the ultraacidic aged ferrihydrite samples (620–830 °C, Figures 5b and 5d). Lack of O_2 release in the near-neutral sample and similar temperature range of evolved HCl in Cumberland and ultraacidic samples (Figures 4 and 5) point to an aquatic system with pH lower than the "acidic pH" range used in these experiments (pH < ~4, Table 1). Under such conditions, both adsorbed perchlorate and chloride are present and evolved O_2 and HCl are comparable to SAM observations of the Cumberland sample. The proposed pH constraint is based on adsorption experiments in which 5.2 mM ClO_4^- and 1.7–12 mM Cl^- were introduced.

Mineralogical and morphological observations indicate that the Sheepbed mudstone was exposed to depositional and postdepositional near-neutral pH conditions. The Sheepbed mudstone was deposited in an ancient lake of near-neutral pH and low salinity which persisted for anywhere from 1,500 to 100,000s of years (Grotzinger et al., 2014; Grotzinger et al., 2015). Solution pH was presumably controlled by aqueous alteration of olivine into saponite and magnetite as evident from low abundances of olivine (1.8 wt.%) and enrichments in smectite (18 wt.%) and magnetite (6 wt.%) (Bristow et al., 2015; Morrison et al., 2018; Vaniman et al., 2014). Postdepositional diagenetic features found in Sheepbed mudstone, including raised ridges, nodules, and light-toned veins filled with calcium sulfate, have also been hypothesized to form at near-neutral to alkaline pH (Fukushi et al., 2019; Gasda et al., 2017; Grotzinger et al., 2014; Léveillé et al., 2014; Schwenzer et al., 2016; Siebach et al., 2014; Stack et al., 2014). A near-neutral aquatic environment would be unfavorable for adsorption of chlorine species of concentration levels up to 5 mM ClO_4^- and 12 mM Cl^-. Acidic events necessary for Cl^- and ClO_4^- adsorption could occur during late stage diagenetic events through interaction with low pH groundwater.

Acidic groundwater has not been previously proposed to come in contact with the Sheepbed sediments. Influxes of acid-sulfate groundwater, however, likely happened in other locations in Gale crater. Acidic groundwater has been proposed as a diagenetic episode in the Murray formation, a fine-grained laminated mudstone, and the stratigraphically lowest unit of the Mount Sharp group (Rampe et al., 2017). Acidic fluids alone or followed by alkaline fluids could also trigger development of the altered fracture zones in the Murray and Stimson formations. The Stimson formation is an eolian sandstone formation that unconformably overlies Murray mudstone (Hausrath et al., 2018; Yen et al., 2017). We, therefore, hypothesize that acidic groundwater was also present during late stages of Sheepbed mudstone diagenesis, perhaps associated with the late stage acidic groundwater diagenesis in the Murray and Stimson formations. The fluid could be a sulfuric acid containing dissolved salts of chloride and perchlorate. Observations of akaganeite in the Cumberland sample support an acidic diagenetic event, perhaps by acid sulfate alteration, as akaganeite can form in the presence of 0.01 to 0.05 M SO_4^{2-} at pH 1.5 (Peretyazhko et al., 2016). Veins filled with calcium sulfate in the Sheepbed mudstone could also have partially formed in such environments since precipitation of $CaSO_4$ is not pH sensitive (Peretyazhko et al., 2018).

The presence of sulfate would not have completely suppressed perchlorate and chloride adsorption (Rietra et al., 2000; Zhang, Brümmer, & Zhang, *1996*). In acid-sulfate alteration environments, sulfate adsorption occurs on positively charged mineral surfaces. Sulfate adsorbs by forming both inner-sphere and outer-sphere complexes on ferrihydrite and akaganeite under acidic conditions (Fukushi et al., 2013; Peretyazhko et al., 2016; Zhu et al., 2013). Sulfate adsorption on Fe (III) (hydr)oxide goethite and Fe (III) (hydr)oxide- and clay-containing soils was lower in the presence of chloride than perchlorate because chloride has higher affinity for surface sites than perchlorate (Rietra et al., 2000; Zhang, Brümmer, & Zhang, *1996*). Although simultaneous adsorption of Cl^-, ClO_4^-, and SO_4^{2-} has not been studied on Fe (III) (hydr)oxides, we hypothesized that the presence of sulfate would not have completely suppressed perchlorate and chloride adsorption based on observations of Rietra et al. (2000) and Zhang, Brümmer, and

Zhang (1996). The minerals with adsorbed chlorine species were likely not exposed to prolonged near-neutral or alkaline groundwater which would lead to desorption of Cl^- and ClO_4^-. The adsorption of perchlorate and chloride might be one of the latest or last aqueous events in the Sheepbed mudstone.

Our experimental results suggested that pH < 4 was required for both perchlorate and chloride to be adsorbed on ferrihydrite in the mudstone. However, it should be noted that larger perchlorate and chloride loadings can lead to larger amounts of adsorbed perchlorate and chloride (Chubar et al., 2005; Kumar et al., 2010). If perchlorate and chloride solution concentrations were increased at near-neutral pH relative to the concentrations used in this work (> > 5-mM ClO_4^- and > > 12-mM Cl^-), then Cl^- and ClO_4^- adsorption levels could theoretically match those at lower pH. Such increase in adsorbed perchlorate and chloride under near-neutral conditions can allow ClO_4^- and Cl^- identification by EGA and extend to higher pH the conditions under which these adsorbed species can be detected in Gale crater. Experimental assessment of adsorption over a wider range of perchlorate and chloride concentrations is necessary to place accurate constraints on pH conditions in ancient aquatic environments in Gale crater.

5. Conclusions

Adsorption of chlorine species (perchlorate and chloride) on freshly synthesized ferrihydrite and akaganeite and on 3-year aged ferrihydrite was investigated, and adsorbed species were characterized with TA/EGA. Our results revealed that 0.2–1.2 wt.% perchlorate was adsorbed within 24 hr on aged and fresh ferrihydrite and akaganeite in ultraacidic (pH 2–2.5) to near-neutral (pH 6.2–7.3) pH range. Chloride was adsorbed (0.5–2 wt.%) on aged and fresh ferrihydrite under ultraacidic and acidic (pH 3.8–4.5) pH conditions, and no chloride adsorption occurred under near-neutral pH. Adsorbed chloride and perchlorate were detectable with EGA. Thermal decomposition of adsorbed perchlorate led to release of O_2 with a well-resolved peak at 306 °C for ferrihydrite and a small peak, tentatively assigned to perchlorate thermal decomposition, at 312 °C for akaganeite which were not observed in the unreacted samples. The evolved HCl was observed in the ultraacidic and acidic aged ferrihydrite samples at >470 °C and originated from adsorbed chloride.

Comparison of EGA results with the data collected by the SAM instrument for the Cumberland drill sample in the Sheepbed mudstone from the Yellowknife Bay area within Gale crater suggested that both adsorbed perchlorate and chloride are present in the mudstone. Evolved O_2 and HCl observed in the mudstone likely originated from perchlorate and chloride adsorbed on ferrihydrite or ferrihydrite-like adsorption phase. Ferrihydrite has been previously proposed to be a part of Fe-rich X-ray amorphous phase(s) in the Sheepbed mudstone. Our study supported this hypothesis and indicated that ferrihydrite in mudstone could be similar to the aged ferrihydrite used in this work. If aquatic conditions in Gale crater were close to our experimental settings (i.e., 5.2 mM ClO_4^- and 1.7 to 12 mM Cl^-), adsorption of both perchlorate and chloride likely occurred under acidic pH < 4 conditions as a result of postdepositional water-rock interactions of ferrihydrite or ferrihydrite-like phase with acid-sulfate groundwater containing dissolved chloride and perchlorate.

References

Acelas, N., & Flórez, E. (2018). Chloride adsorption on Fe-and Al-(hydr) oxide: Estimation of Gibbs free energies. *Adsorption*, *24*(3), 243–248.

Archer, P. D., Franz, H. B., Sutter, B., Arevalo, R. D., Coll, P., Eigenbrode, J. L., et al. (2014). Abundances and implications of volatile-bearing species from evolved gas analysis of the Rocknest aeolian deposit, Gale Crater, Mars. *Journal of Geophysical Research: Planets*, *119*, 237–254. https://doi.org/10.1002/2013JE004493

Berger, J. A., Schmidt, M. E., Gellert, R., Campbell, J. L., King, P. L., Flemming, R. L., et al. (2016). A global Mars dust composition refined by the Alpha-Particle X-ray Spectrometer in Gale crater. *Geophysical Research Letters*, *43*, 67–75. https://doi.org/10.1002/2015GL066675

Bourikas, K., Hiemstra, T., & Van Riemsdijk, W. (2001). Ion pair formation and primary charging behavior of titanium oxide (anatase and rutile). *Langmuir*, *17*(3), 749–756.

Bristow, T. F., Bish, D. L., Vaniman, D. T., Morris, R. V., Blake, D. F., Grotzinger, J. P., et al. (2015). The origin and implications of clay minerals from Yellowknife Bay, Gale crater, Mars. *American Mineralogist*, *100*(4), 824–836. https://doi.org/10.2138/am-2015-5077CCBYNCND

Chambaere, D. G., & Degrave, E. (1984). A study of the non-stoichiometrical halogen and water content of β-FeOOH. *Physica Status Solidi a-Applied Research*, *83*(1), 93–102.

Chubar, N., Samanidou, V., Kouts, V., Gallios, G., Kanibolotsky, V., Strelko, V., & Zhuravlev, I. (2005). Adsorption of fluoride, chloride, bromide, and bromate ions on a novel ion exchanger. *Journal of Colloid and Interface Science*, *291*(1), 67–74. https://doi.org/10.1016/j.jcis.2005.04.086

Clark, J., Sutter, B., McAdam, A., Rampe, E., Archer, P., Ming, D., et al. (2019). High-temperature HCl evolutions from mixtures of perchlorates and chlorides with water-bearing phases: Implications for the Sample Analysis at Mars (SAM) instrument in Gale crater, Mars. *Journal of Geophysical Research: Planets*, *125*. https://doi.org/10.1029/2019JE006173

Cornell, R., & Schwertmann, U. (2003). The iron oxides: Structure, properties, reactions, occurrence and uses, VCH.

Dehouck, E., McLennan, S. M., Meslin, P. Y., & Cousin, A. (2014). Constraints on abundance, composition, and nature of X-ray amorphous components of soils and rocks at Gale crater, Mars. *Journal of Geophysical Research: Planets*, *119*, 2640–2657.

Dultz, S., Behrens, H., Helsch, G., & Deubener, J. (2016). Electrolyte effects on surface chemistry of basaltic glass in the initial stages of dissolution. *Chemical Geology*, *426*, 71–84.

Dumont, F., & Watillon, A. (1971). Stability of ferric oxide hydrosols. *Discussions of the Faraday Society*, *52*, 352–360.

Fischer, W., & Schwertmann, U. (1975). The formation of hematite from amorphous iron (III) hydroxide. *Clays and Clay Minerals*, *23*(1), 33–37.

Fukushi, K., Aoyama, K., Yang, C., Kitadai, N., & Nakashima, S. (2013). Surface complexation modeling for sulfate adsorption on ferrihydrite consistent with in situ infrared spectroscopic observations. *Applied Geochemistry*, *36*, 92–103.

Fukushi, K., Sekine, Y., Sakuma, H., Morida, K., & Wordsworth, R. (2019). Semiarid climate and hyposaline lake on early Mars inferred from reconstructed water chemistry at Gale. *Nature Communications*, *10*(1), 1–11.

Gasda, P. J., Haldeman, E. B., Wiens, R. C., Rapin, W., Bristow, T. F., Bridges, J. C., et al. (2017). In situ detection of boron by ChemCam on Mars. *Geophysical Research Letters*, *44*, 8739–8748. https://doi.org/10.1002/2017GL074480

Glavin, D. P., Freissinet, C., Miller, K. E., Eigenbrode, J. L., Brunner, A. E., Buch, A., et al. (2013). Evidence for perchlorates and the origin of chlorinated hydrocarbons detected by SAM at the Rocknest aeolian deposit in Gale Crater. *Journal of Geophysical Research: Planets*, *118*, 1955–1973. https://doi.org/10.1002/jgre.20144

Grotzinger, J., Gupta, S., Malin, M., Rubin, D., Schieber, J., Siebach, K., et al. (2015). Deposition, exhumation, and paleoclimate of an ancient lake deposit, Gale crater, Mars. *Science*, *350*(6257), aac7575.

Grotzinger, J. P., Sumner, D. Y., Kah, L. C., Stack, K., Gupta, S., Edgar, L., et al. (2014). A habitable fluvio-lacustrine environment at Yellowknife Bay, Gale Crater, Mars. *Science*, *343*(6169), 1,242,777.

Hausrath, E. M., Ming, D., Peretyazhko, T., & Rampe, E. (2018). Reactive transport and mass balance modeling of the Stimson sedimentary formation and altered fracture zones constrain diagenetic conditions at Gale crater, Mars. *Earth and Planetary Science Letters*, *491*, 1–10.

Hiemstra, T., & Van Riemsdijk, W. H. (2009). A surface structural model for ferrihydrite I: Sites related to primary charge, molar mass, and mass density. *Geochimica et Cosmochimica Acta*, *73*(15), 4423–4436.

Hogancamp, J., Sutter, B., Morris, R., Archer, P., Ming, D., Rampe, E., et al. (2018). Chlorate/Fe-bearing phase mixtures as a possible source of oxygen and chlorine detected by the sample analysis at Mars instrument in Gale Crater, Mars. *Journal of Geophysical Research: Planets*, *123*, 2920–2938. https://doi.org/10.1029/2018JE005691

Hsi, C.-K. D., & Langmuir, D. (1985). Adsorption of uranyl onto ferric oxyhydroxides: Application of the surface complexation site-binding model. *Geochimica et Cosmochimica Acta*, *49*(9), 1931–1941.

Kosmulski, M. (2002). The pH-dependent surface charging and the points of zero charge. *Journal of Colloid and Interface Science*, *253*(1), 77–87. https://doi.org/10.1006/jcis.2002.8490

Kozin, P. A., & Boily, J.-F. (2013). Proton binding and ion exchange at the akaganeite/water interface. *The Journal of Physical Chemistry C*, *117*(12), 6409–6419.

Kumar, E., Bhatnagar, A., Choi, J.-A., Kumar, U., Min, B., Kim, Y., et al. (2010). Perchlorate removal from aqueous solutions by granular ferric hydroxide (GFH). *Chemical Engineering Journal*, *159*(1–3), 84–90.

Kumar, E., Bhatnagar, A., Hogland, W., Marques, M., & Sillanpää, M. (2014). Interaction of inorganic anions with iron-mineral adsorbents in aqueous media—A review. *Advances in Colloid and Interface Science*, *203*, 11–21. https://doi.org/10.1016/j.cis.2013.10.026

Léveillé, R. J., Bridges, J., Wiens, R. C., Mangold, N., Cousin, A., Lanza, N., et al. (2014). Chemistry of fracture-filling raised ridges in Yellowknife Bay, Gale Crater: Window into past aqueous activity and habitability on Mars. *Journal of Geophysical Research: Planets*, *119*, 2398–2415. https://doi.org/10.1002/2014JE004620

Li, Y., Xu, T., Cui, C., & Li, Y. (2015). The adsorption of chlorite and chlorate by calcium carbonate in a drinking water pipe network. *Desalination and Water Treatment*, *53*(7), 1881–1887.

Lien, H.-L., Yu, C. C., & Lee, Y.-C. (2010). Perchlorate removal by acidified zero-valent aluminum and aluminum hydroxide. *Chemosphere*, *80*(8), 888–893. https://doi.org/10.1016/j.chemosphere.2010.05.013

Luna, C., Ilyn, M., Vega, V., Prida, V. M., González, J. N., & Mendoza-Reséndez, R. (2014). Size distribution and frustrated antiferromagnetic coupling effects on the magnetic behavior of ultrafine akaganéite (β-FeOOH) nanoparticles. *The Journal of Physical Chemistry C*, *118*(36), 21,128–21,139.

Mahmudov, R., & Huang, C. P. (2011). Selective adsorption of oxyanions on activated carbon exemplified by Filtrasorb 400 (F400). *Separation and Purification Technology*, *77*(3), 294–300.

Mazeina, L., Deore, S., & Navrotsky, A. (2006). Energetics of bulk and nano-akaganeite, β-FeOOH: Enthalpy of formation, surface enthalpy, and enthalpy of water adsorption. *Chemistry of Materials*, *18*(7), 1830–1838.

Meunier, A. (2005). *Clays*. Berlin: Springer Science & Business Media.

Ming, D. W., Gellert, R., Morris, R. V., Arvidson, R. E., Brueckner, J., Clark, B. C., et al. (2008). Geochemical properties of rocks and soils in Gusev crater, Mars: Results of the Alpha Particle X-ray Spectrometer from Cumberland Ridge to Home Plate. *Journal of Geophysical Research*, *113*, E12S39. https://doi.org/10.1029/2008JE003195

Ming, D. W., Archer Jr., P. D., Glavin, D. P., Eigenbrode, J. L., Franz, H. B., Sutter, B., et al., & MSL Science Team (2014). Volatile and organic compositions of sedimentary rocks in Yellowknife Bay, Gale Crater, Mars. *Science*, *343*(6169), 1,245,267.

Morris, R. V., Klingelhoefer, G., Bernhardt, B., Schröder, C., Rodionov, D. S., De Souza, P. A., et al. (2004). Mineralogy at Gusev Crater from the Mössbauer spectrometer on the Spirit Rover. *Science*, *305*(5685), 833–836.

Morrison, S. M., Downs, R. T., Blake, D. F., Vaniman, D. T., Ming, D. W., Hazen, R. M., et al. (2018). Crystal chemistry of martian minerals from Bradbury Landing through Naukluft Plateau, Gale crater, Mars. *American Mineralogist*, *103*(6), 857–871.

Parida, K., Gorai, B., Das, N., & Rao, S. (1997). Studies on ferric oxide hydroxides: III. Adsorption of selenite (SeO2− 3) on different forms of iron oxyhydroxides. *Journal of Colloid and Interface Science*, *185*(2), 355–362. https://doi.org/10.1006/jcis.1996.4522

Peretyazhko>, T. S., Ming, D. W., Rampe, E. B., Morris, R. V., & Agresti, D. G. (2018). Effect of solution pH and chloride concentration on akaganeite precipitation: Implications for akaganeite formation on Mars. *Journal of Geophysical Research: Planets*, *123*, 2211–2222. https://doi.org/10.1029/2018JE005630

Peretyazhko, T. S., Fox, A., Sutter, B., Niles, P. B., Adams, M., Morris, R. V., & Ming, D. W. (2016). Synthesis of akaganeite in the presence of sulfate: Implications for akaganeite formation in Yellowknife Bay, Gale Crater, Mars. *Geochimica et Cosmochimica Acta*, *188*, 284–296.

Peretyazhko, T. S., Niles, P. B., Sutter, B., Morris, R. V., Agresti, D. G., Le, L., & Ming, D. W. (2018). Smectite formation in the presence of sulfuric acid: Implications for acidic smectite formation on early Mars. *Geochimica et Cosmochimica Acta*, *220*, 248–260.

Peretyazhko, T. S., Pan, M. J., Ming, D. W., Rampe, E. B., Morris, R. V., & Agresti, D. G. (2019). Reaction of akaganeite with Mars-relevant anions. *ACS Earth and Space Chemistry*, *3*(2), 314–323. https://doi.org/10.1021/acsearthspacechem.8b00173

Rampe, E. B., Ming, D. W., Blake, D. F., Bristow, T. F., Chipera, S. J., Grotzinger, J. P., et al. (2017). Mineralogy of an ancient lacustrine mudstone succession from the Murray formation, Gale crater, Mars. *Earth and Planetary Science Letters*, *471*, 172–185. https://doi.org/10.1016/j.epsl.2017.04.021

Rietra, R., Hiemstra, T., & Van Riemsdijk, W. (2000). Electrolyte anion affinity and its effect on oxyanion adsorption on goethite. *Journal of Colloid and Interface Science*, *229*(1), 199–206. https://doi.org/10.1006/jcis.2000.6982

Schwenzer, S. P., Bridges, J. C., Wiens, R. C., Conrad, P. G., Kelley, S., Leveille, R., et al. (2016). Fluids during diagenesis and sulfate vein formation in sediments at Gale crater, Mars. *Meteoritics & Planetary Science*, *51*(11), 2175–2202.

Schwertmann, U., Friedl, J., & Stanjek, H. (1999). From Fe (III) ions to ferrihydrite and then to hematite. *Journal of Colloid and Interface Science*, *209*(1), 215–223. https://doi.org/10.1006/jcis.1998.5899

Shimada, S. (1992). Acoustic emission in the process of dehydration and thermal decomposition of $NaClO_4 \cdot H_2O$. *Thermochimica Acta*, *196*(2), 237–246.

Siebach, K., Grotzinger, J., Kah, L., Stack, K., Malin, M., Léveillé, R., & Sumner, D. (2014). Subaqueous shrinkage cracks in the Sheepbed mudstone: Implications for early fluid diagenesis, Gale crater, Mars. *Journal of Geophysical Research: Planets*, *119*, 1597–1613. https://doi.org/10.1002/2014JE004623

Smith, S. J., Page, K., Kim, H., Campbell, B. J., Boerio-Goates, J., & Woodfield, B. F. (2012). Novel synthesis and structural analysis of ferrihydrite. *Inorganic Chemistry*, *51*(11), 6421–6424. https://doi.org/10.1021/ic300937f

Soltis, J. A., Feinberg, J. M., Gilbert, B., & Penn, R. L. (2016). Phase transformation and particle-mediated growth in the formation of hematite from 2-line ferrihydrite. *Crystal Growth & Design*, *16*(2), 922–932.

Sparks, D. L. (2003). *Environmental soil chemistry*. London: Academic Press.

Stack, K., Grotzinger, J., Kah, L., Schmidt, M., Mangold, N., Edgett, K., et al. (2014). Diagenetic origin of nodules in the Sheepbed member, Yellowknife Bay formation, Gale crater, Mars. *Journal of Geophysical Research: Planets*, *119*, 1637–1664. https://doi.org/10.1002/2014JE004617

Ståhl, K., Nielsen, K., Jiang, J., Lebech, B., Hanson, J. C., Norby, P., & van Lanschot, J. (2003). On the akaganéite crystal structure, phase transformations and possible role in post-excavational corrosion of iron artifacts. *Corrosion Science*, *45*(11), 2563–2575.

Sutter, B., Heil, E., Morris, R., Archer, P., Ming, D., Niles, P., et al. (2015). The investigation of perchlorate/iron phase mixtures as a possible source of oxygen detected by the Sample Analysis at Mars (SAM) instrument in Gale Crater, Mars. *Lunar and Planetary Science Conference abstract*.

Sutter, B., Mcadam, A. C., Mahaffy, P. R., Ming, D. W., Edgett, K. S., Rampe, E. B., et al. (2017). Evolved gas analyses of sedimentary rocks and eolian sediment in Gale crater, Mars: Results of the curiosity Rover's Sample Analysis at Mars (SAM) instrument from Yellowknife Bay to the Namib Dune. *Journal of Geophysical Research: Planets*, *122*, 2574–2609. https://doi.org/10.1002/2016JE005225

Torrent, J., Guzman, R., & Parra, M. (1982). Influence of relative humidity on the crystallization of Fe (III) oxides from ferrihydrite. *Clays and Clay Minerals*, *30*(5), 337–340.

Vaniman, D. T., Bish, D. L., Ming, D. W., Bristow, T. F., Morris, R. V., Blake, D. F., et al. (2014). Mineralogy of a mudstone at Yellowknife Bay, Gale crater, Mars. *Science*, *343*(6169), 1,243,480.

Wang, P., Ji, G., & Yu, T. (1987). Adsorption of chloride and nitrate by variable charge soils in relation to the electric charge of the soil. *Zeitschrift für Pflanzenernährung und Bodenkunde*, *150*(1), 17–23.

Yen, A., Ming, D., Vaniman, D., Gellert, R., Blake, D., Morris, R., et al. (2017). Multiple stages of aqueous alteration along fractures in mudstone and sandstone strata in Gale Crater, Mars. *Earth and Planetary Science Letters*, *471*, 186–198.

Zhang, G., Brümmer, G., & Zhang, X. (1996). Effect of perchlorate, nitrate, chloride and pH on sulfate adsorption by variable-charge soils. *Geoderma*, *73*(3–4), 217–229.

Zhang, Y., Kshirsagar, G., Ellison, J. E., & Cannon, J. C. (1996). Catalytic effects of metal oxides on the decomposition of Potassium perchlorate. *Thermochimica Acta*, *278*, 119–127.

Zhu, M., Northrup, P., Shi, C., Billinge, S. J., Sparks, D. L., & Waychunas, G. A. (2013). Structure of sulfate adsorption complexes on ferrihydrite. *Environmental Science & Technology Letters*, *1*(1), 97–101.